Classification: Major - Biological Sciences; Minor - Neuroscience

Figure-ground modulation in awake primate thalamus

Helen E Jones[a]*, Ian M Andolina[a], Stewart D Shipp[a], Daniel L Adams[b], Javier Cudeiro[c], Thomas E Salt[a], Adam M Sillito[a]

[a] Department of Visual Neuroscience, UCL Inst. of Ophthalmology, 11-43 Bath Street, London EC1V 9EL, United Kingdom.

[b] Beckman Vision Center, University of California, 10 Koret Way, San Francisco, CA 94143, USA.

[c] Department of Medicine – Neurocom and INIBIC (Institute of Biomedical Research of A Coruña), University of A Coruña, Campus de Oza, s/n 15006, A Coruña, Spain

* Corresponding author: H E Jones, Dept. of Visual Neuroscience, UCL Inst. of Ophthalmology, 11-43 Bath Street, London EC1V 9EL. United Kingdom.

Tel: +44 (0)20 76086844, E-mail: hjones@ioores.co.uk

Keywords: vision, perception, feedback figure-ground discrimination, lateral geniculate nucleus

Abstract

Figure-ground discrimination refers to the perception of an object, the figure, against a nondescript background. Neural mechanisms of figure-ground detection have been associated with feedback interactions between higher centers and primary visual cortex, and held to index the impact of global analysis upon local feature encoding. Here, in recordings from visual thalamus of alert primates, we demonstrate a robust enhancement of neuronal firing when the figure, as opposed to the ground, component of a motion-defined figure-ground stimulus is located over the receptive field. In this paradigm, visual stimulation of the receptive field and its near environs is identical across both conditions suggesting that the response enhancement reflects higher integrative mechanisms. It thus appears that cortical activity generating the higher order percept of the figure is simultaneously re-entered into the lowest level that is anatomically possible – the thalamus – so that the signature of the evolving representation of the figure is imprinted on the input driving it, in an iterative process.

Significance Statement

Perceptually, the visual cortical areas are considered to reconstruct objects from the diverse components of early distributed processing by grouping image elements and segregating them from the background as a figure. An assumption here is that raw, essentially unchanged information from the visual thalamus provides the basic pattern essential for the operation of these higher-level abstractions. However, here we demonstrate strong enhancement of neuronal firing to the figure component of a figure-ground stimulus in recordings from the visual thalamus of behaving primates. This suggests that the signature

of a higher order percept is introduced into the thalamus in a re-entrant manner via the corticofugal feedback connections, and causes our visual input to confirm what we think we are seeing.

\body

Introduction

Classically our percept of the world and the objects in it is considered to derive from a collation of the information from the sensory periphery, relayed via the sensory thalamic nuclei to the cortex, where salient features are detected and integrated across spatial and modality domains to generate our ongoing perception. Thus, in vision, the retinal input to the visual thalamus is relayed to the visual cortex where the cortical circuitry assembles the components of the input into configurations that detect feature orientation and direction of motion. Further processing in the cortical circuitry beyond the primary visual cortex then provides the integration to reflect objects and objects distinguished from background. In figure-ground discrimination our visual system reconstructs objects from the diverse components of early distributed processing by grouping image elements and segregating them from the background as a figure. In this view the neural mechanisms of figure-ground detection are linked to processes operating in primary and higher visual cortical areas (1-6) and the assumption is that relatively inviolate information from the visual thalamus provides the raw substructure essential for the veracity of these higher level abstractions. However, another feature of the organization of sensory systems and the visual system is that the feedforward pathways are paralleled by extensive feedback pathways (7-9). Moreover this feedback is reflected all the way back to the sensory thalamic nuclei and in the visual system certainly, is very fast (7). What does this serve? It might logically be

conjectured to be just gain control, but various studies suggest that there may be more to it (7, 9-16). The question is what? It would seem surprising that the signature of the higher level cortical process is reflected in the visual thalamus, but it needs to be tested. Here, we consider the possibility that the high level representation of the signal distinguishing a figure from ground might, because of the feedback connections, be reflected in the activity seen in neurons in the lateral geniculate nucleus (LGN) of the visual thalamus. This has neither been previously tested nor reported, and if true would change how we view the mechanisms underpinning some aspects of the higher level integration.

We have used the salient appearance of a figure defined by motion contrast, posited by neurocomputational models to depend upon interactions amongst areas V5/MT, V2 and V1 (17, 18). These modeling approaches have proposed two complementary processes, one driven by detection of feature discontinuities establishing contour boundaries and the other a region filling in mechanism that links the representation of the common features in the figure (1, 2, 5). These processes have previously been linked to mechanisms operating in primary and higher cortical areas, and suggested to involve feedback to amplify the neural response in the region representing the center of the figure (3, 4, 6, 19, but see 20). The key to the tests in the experimental design, exploited here, and for earlier studies of cortical responses to figure-ground stimuli (3, 6, 21), is that the visual stimulation of the test receptive field (RF) and its near environs is identical across the 'figure' and 'ground' conditions; and the figure condition is determined by a change remote to the LGN cell classical RF. Hence any difference in LGN activation should be attributable to higher mechanisms integrating events over a larger spatial scale and feeding the information back down the system. This deduction is doubly warranted in our case, when the figure border is

defined by motion contrast, and neural directional mechanisms in macaque monkey are generally accepted to be neither intrinsic to the retina, nor LGN, but first developed in area V1 (22, 23) (although note ref. (24) and also see Results).

Results

The stimulus was a pattern of randomized drifting dots with the figure pop-out delineated by the opposite direction of motion of the dots within the figure and the ground (Figure 1A-1B and see Materials and Methods). Two macaque monkeys were trained to fixate centrally within a large 30° static random dot field. Following a fixation period of at least 0.4s, dot motion commenced to define a square figure at one of four pseudorandom screen locations and the monkeys were trained to saccade to and re-fixate at the figure center within 500ms of motion onset. Psychophysically, this is an exercise in exogenous ('bottom-up') attentional capture (25), for the monkeys had no cue, and no means of predicting the figure location, that was equally frequent across the four sites.

Our results are based on recordings from 77 single unit (S) and 63 multi unit (Mu) recordings. As similar response patterns were observed for both unit types, data for both are pooled. Our single unit population sample largely comprised parvocellular cells although we also obtained some recordings from koniocellular and magnocellular cells. Across the single unit data, similar results were observed across the three cell groups (see Fig. 2) and data for all cell types were therefore pooled. The RFs of parafoveal LGN cells were located centrally within the figure region for one of these figure locations and remote from the figure border. The standard figure size was 3 to 4° (3° ± 0.82 SD n = 140), but was made smaller for fields within 5° of the fovea (though never less than 2°, see Materials and

Methods). We routinely used all pairings of rightward and leftward dot motion between figure and ground thus (as noted above) exposing the RF to the identical set of local features across 'figure' and 'ground' trials (the latter being, necessarily, three times more frequent). Many LGN cells responded weakly or not at all to the ground stimulus (Figs. 1C-F, Fig. 2) although some showed a small onset transient (See Fig. S2A for an example). This itself was surprising because it suggests that there is at most a low input to the cortex from these cells in this situation. Whilst it is consistent with previous work reporting the presence of strong surround suppressive effects in the LGN (11, 26-28) it may also in part reflect a failure of the small LGN cell receptive fields to distinguish between the static and moving noise patterns because of ongoing motion secondary to residual eye movements. However this lack of response contrasted with the fact that we observed a strong, long latency (median onset latency 90ms ± 2.26 SE, n = 140) increase in firing rate to the figure stimulus (Figs. 1C-F, Fig. 2). To quantify this enhancement, we calculated a figure-ground modulation index value (FGM) for each cell by taking the difference between the averaged responses to the figure and ground conditions normalized with respect to the sum of the averaged responses to the figure and ground (see Materials and Methods). We adopted the same analysis strategies previously used in V1 (29) (where neurons commonly exhibit strongly orientation and direction selective responses) to ensure that any potential confound arising from the weak directional biases previously reported for some macaque LGN cells (24) were controlled for (see Materials and Methods). There was a marked figure-ground modulation of the response across our sample (median enhancement above ground 56% ± 6.07 SE, n = 140). We illustrate this by the average population responses (Fig. 2A, see also Fig. S3), the distribution of FGM values across our sample (Fig. 2B) and by the comparison

of responses evoked by ground versus figure stimuli (Figs. 2C-D). Approximately 90% of cells (128 out of 140) showed a FGM index of 20% or more.

Having discovered such a pronounced response to the figure center, we wondered if the response at the border might be further enhanced, as observed in V1 (albeit with a non-identical behavioral paradigm, and with a static, textural mode of figure-ground delineation - (6)); border detection is a key process in 'filling-in' models of figural discrimination, essentially setting the topographic boundaries of a neural map filled in by the figural surface features (1, 2, 5). In a subset of cells (n = 37), we also checked the effect of displacing the figure location so that the border between the figure and ground components of the stimulus was located over the RF, interlacing figure, border and ground trials in a pseudorandom sequence, as before. There was however no significant difference in either the magnitude or onset latency of the responses evoked by figure and border location stimuli ($P = 0.379$ and $P = 0.795$ respectively, Wilcoxon matched pairs test, n = 37, Fig. 3). There were actually two distinct borders in our stimulus configuration, where the opposite directions of dot motion were either perpendicular, or parallel to the edge of the square-shaped figure; we tested both, but noted no qualitative differences and pooled the two conditions for the population average data in Fig. 3C.

Our data clearly demonstrate that LGN neurons show differential spiking activity for figure compared to ground stimulation conditions in a manner analogous to the figure-ground modulation previously reported for cortical stages of the visual hierarchy. However, as the task design required the monkey to saccade to the figure, an alternative interpretation could be that a component of the neuronal enhancement in our behavioral paradigm reflected pre-saccadic activation. In order to explore this, we also recorded the

responses of a number of LGN neurons whose RFs were located in very close proximity to the fovea. In these cases, a figure stimulus located over the RF also encompassed the fixation window and the monkeys were rewarded simply for maintaining fixation when the figure was located over the RF. Although the monkey did not make a saccade to the figure stimulus overlying the RF, we continued to observe the strong, long latency increase in firing rate to the figure stimulus (Fig. 4) with a marked figure-ground modulation of the response across the sample (median enhancement above ground 59% ± 8.42 SE, n = 20).

Discussion

Our results show that the responses of LGN cells in awake behaving monkeys can be strongly modulated by a motion defined figure-ground stimulus. In a sense this is unexpected, given that it is generally accepted that neither contour orientation, nor spatiotemporal direction of drift are explicitly represented at this level. Our results were observed with figure sizes notably larger (our standard figure sizes were 3 to 4°) than the LGN cells' RF diameter (0.75^{o} ± 0.79 SD, n = 140). Thus the figure-ground modulation we saw was for RFs that were located centrally within the figure region and remote from the figure border. This is commensurate with the results from virtually all the studies in V1 and V2 (3, 6, 21) although one study in V1 (20) only observed a modulation when the border was close to the RF. The discrepancy in this latter case has been linked to task design (3, 6, 20, 21) so it is relevant to note that our task design closely mirrored that of the former studies rather than the latter. We believe the effect we have observed closely matches the characteristics of figure-ground modulation in the cortex and reflects the influence of feedback circuitry integrating cortical and thalamic levels. The results thus

suggest that the signature of a higher order percept is fed back into the thalamus in a re-entrant manner, changing the information relayed to the cortex. This implies that this re-alignment of the sensory input from the thalamus, to reflect the percept initially integrated at higher cortical levels, is an important component of the neural logic to the process extracting and testing the ever changing features of the visual world. This new observation argues for a re-evaluation of the iterative neural mechanisms that represent and extract salient features of the visual world.

A striking feature of our data is the magnitude of the modulation to the figure condition. It contrasted strongly with the minimal response shown by many of the cells to the motion of the background stimulus in isolation. We believe it is consistent with a system that relays minimal information to a "non-salient stimulus" (7, 11), and that the "global" salience detected by higher level feature detectors, sampling larger areas of visual space, is fed back and modulates the response to the underlying retinal excitatory input to the LGN cells, by dis-inhibition and direct facilitation. A few cells (eg Fig. S2A) did give a transient response to the onset of stimulus motion and these might serve to prime the cortex also, but the major point seems to be a feedback driven "release" of excitatory drive initiated from retinotopic locations way beyond the LGN cell receptive field, with a most logical origin in MT. Feedback from MT has been shown to exert a strong influence on the earliest component of the response of V1 cells to both moving and flashing stimuli (19) and strong effects on LGN cell responses exerted from locations outside their receptive field (30).

The modulatory effect reported here greatly exceeds that observed by us or any other group for modulation of LGN cell responses by classical, extra-classical or remote

stimuli (7, 16, 31-34). It has long been acknowledged that the responses of many neurons in the visual system can be influenced by stimuli remote from the classical RF (31). A variety of effects have been reported in anesthetized animals. These range from non-specific inhibitory or facilitatory effects such as "shift" or "periphery" effects predominantly linked to retinal and geniculate cell responses, to direction and orientation selective contextual effects most commonly linked to V1 and higher cortical areas such as area MT (31, 35-38). These latter stimulus specific contextual modulatory effects have been extensively linked to a role in local-global comparisons and in the discrimination of figure from background (29, 31, 38). A range of studies in awake behaving monkey has linked mechanisms underlying figure-ground detection to processes operating in V1 and higher cortical areas (3, 6, 21, 29). However our study is the first to demonstrate, in awake behaving monkey, the presence of differential spiking activity for figure compared to ground stimulation conditions in the LGN that is analogous to the figure-ground modulatory effects previously demonstrated only for cortical stages of the visual hierarchy (3, 6, 21, 29). As the magnitude of the effect we observed is substantially larger than that reported for any of the previous studies of contextual modulatory effects in the LGN (7, 16, 32-34) it suggests that it draws on processes that are enhanced or only enabled in the behaving preparation.

As the speeded reaction time task design we deployed (39) required the monkey to saccade to the figure, an alternative interpretation for the differential effects we observed could be that a component of the neuronal enhancement in our behavioral paradigm reflected pre-saccadic activation. Although the current literature regarding perisaccadic modulatory effects in LGN would argue against the latter interpretation (40) we also

obtained direct evidence against a motor-based, pre-saccadic interpretation by recording from cells with foveal or perifoveal fields. Robust FGM responses were still observed despite the monkey completing the task without making a saccade to the figure stimulus overlying the RF (Fig. 4), a result that directly argues against the modulation being pre-saccadic in origin. We have also recorded preliminary data from a limited sample of neurons using an alternative approach to probe this issue. Essentially, we added a second, identical target figure to our standard figure-ground task and rewarded the monkey for making a saccade to the location of either figure. The monkey could thus choose to saccade to either target as both were rewarded but the natural preference was to select the target closer to the fixation point (41). By varying the position of the second target, this design allowed us to compare the response to an identical stimulus situated over the neuron's RF when it was or was not the target for a saccade. Although the FGM magnitude was significantly smaller when the figure overlying the RF was not the target for a saccade compared to when it was the saccade target ($P = 0.005$, Wilcoxon matched pairs test, n = 14), we nonetheless continued to observe a long latency increase in firing to the figure stimulus overlying the RF even in this condition (Fig. S2B). There was a significant difference ($P < 0.001$, Friedman ANOVA, n = 14), in the magnitude of the evoked responses to the different stimulus conditions, and the responses to the figure stimulus for both saccade conditions were significantly larger than those to the ground stimulus ($P < 0.05$, post-hoc Wilcoxon tests using Bonferroni correction). Again, this data argues against the interpretation that the effects were wholly dependent on detecting and making a saccade to a target stimulus overlying the RF.

It seems clear that the FGM effect we have observed must contribute to the salience of the figure because it amplifies the strength of the ongoing input from the LGN to the cortex for the figure. Given the magnitude of the effect it might also index an attentional mechanism driven by feedback (42), again though one which highlights salience, but this will require further examination as our paradigm could not distinguish between exogenously captured attention directed towards the RF and figure-ground modulation. Studies in V1 have shown separate phases of activity, relating to figure-ground separation, and a subsequent attentional modulation. These have been timed at approximately 60 and 140 ms respectively, using a similar dot motion defined figure (43). A psychophysical study of the tradeoff between dot-speed and presentation time revealed that for human perception there was a time constant an order of magnitude larger for detecting a figure defined by dot motion, as opposed to luminance (44). The median latency we recorded in LGN, of 90 ms, is benchmarked by the average saccadic RT of our monkeys – 190 ms – and by the latency to motion onset in area V5/MT, that is contingent on dot-speed, but estimated (under anesthesia) at 72 ms for our speed of 4^{o}/s (45). Thus we infer that re-entry from V5/MT, via V1, is a plausible mechanism for motion-defined FGM in the LGN, further highlighting the potential for dynamic interplay between stations along the neuraxis of motion processing (7). Indeed, we have recently shown that feedback from V5/MT, in the anesthetized monkey, is able to influence the responses of LGN neurons to moving stimuli originating from spatial foci substantially beyond their classical RF (30), further underlining its potential role in mediating the motion defined FGM we report here. Earlier work in anesthetized macaques has also demonstrated the potential contribution of corticogeniculate feedback from V1 to the LGN to extra-classical RF responses (11, 16)

further underlining the likely role of feedback mechanisms to these effects. Again the interesting difference with the current data is the magnitude of the effect we observed here.

Although thalamic relay nuclei have traditionally been regarded as simple sensory relays to the primary sensory cortex, there is a large body of evidence that now suggests cortical feedback connections to the thalamus can influence the transmission of information through it in a functionally selective manner (7, 9, 14). These feedback connections allow for the abstract of the higher level cortical processes to be fed back into the LGN, with a weighting linked to behavioral salience and attention. Probing these issues to reveal such influences requires a reappraisal of the response characteristics of LGN cells based on their responses to classes of visual stimuli and behavioral task more commonly linked to the analysis of higher-level visual function (30, 42). This we have attempted here, and believe our observations underline the fact that the visual thalamus is essentially embedded in the cortical circuitry and should be seen thus, rather than as forming a distinct input stage serving only to relay information up the system. These new observations, together with other preceding work in the field (7, 30, 42, 46, 47), also contain the implication that on a moment by moment basis, the input to the visual cortex from the thalamus is refined to reflect what the system as a whole (7, 9) considers to be the stimulus engaging its input, rather than simply what the component input channels would indicate in isolation.

Materials and Methods

All procedures were carried out in accordance with the Animals (Scientific Procedures) Act 1986 and were approved by the local ethical committee at UCL's Inst. of Ophthalmology and by the UK Home Office. Two naïve male Macaca mulatta monkeys, each weighing 7

to 9 kg, were trained, using solely positive reinforcement techniques in accordance with the Prescott review recommendations, to voluntarily enter a Crist Instrument primate chair and habituated to the laboratory environment. Surgical procedures and extracellular recording methods are described in SI Experimental Procedures.

Visual stimulation and behavioral tasks. Visual stimuli were generated in Matlab (Mathworks Inc.) using the Psychophysics toolbox running a custom stimulus-generator (http://dx.doi.org/10.5281/zenodo.11080). See SI, Experimental Procedures for further details. Prior to any recording, animals were trained to the laboratory environment by sitting comfortably under head fixation. Next, animals were trained using fluid reward, in conjunction with fluid control where necessary, to view the monitor binocularly and to maintain fixation for 2-3 seconds within a 1° radius fixation window around a red fixation spot subtending 0.2° visual angle; eye position was monitored using an Eyelink 1000 infra-red eyetracker (SR Research Ltd) recording at 250Hz. During this fixation period we presented a range of RF isolating stimuli (see below) para-foveally; this enabled us to locate and identify RFs of LGN cells for further study during experimental recording sessions. Animals were subsequently trained in the main figure-ground experimental task. Again, stimuli were presented under binocular viewing conditions and animals were trained to initiate fixation within a 1° radius fixation window around a yellow fixation spot presented against a static full screen random dot display for at least 0.4 seconds (though in general the monkeys fixated much more precisely on the fixation spot, see Fig. S2C). Once the fixation criteria were met, motion initiated, and both the figure and ground random dot stimuli moved in opposite directions. To complete the task successfully and receive a drop

of preferred fruit juice, the animal had to saccade to the location of the figure within 500 ms of stimulus motion onset. Saccades were identified on the basis of their velocity and acceleration.

During recording sessions, prior to running the figure-ground experimental task, we ran a battery of preliminary tests using a range of RF isolating stimuli, including a range of contrast, chromatic and opponent defined stimuli, to determine RF location and physiological response properties (11, 26, 30, 42). We used these RF characterizations (specifically size, opponency and chromaticity, monocularity), along with stereotypical shifts in eye preference and classical retinotopic progression through penetration depth (48, 49), and the 3D chamber co-ordinate reconstructions of the MRI, to ensure our sampling was confined to the LGN. Cells were categorized as parvocellular, magnocellular and koniocellular based on physiological response properties, electrode depth and stereotypical shifts in eye preference (11, 26, 30, 42). In order to ensure that one location of the figure stimulus was accurately located over the RF center, the location and extent of the RF was carefully assessed using a range of stimuli including flashing spots (or bars) of light, drifting bars and/or edges and patches of sinusoidal grating. In particular, we documented the location and spatial extent of the RF center by exploring the spatial distribution of locations from which a contrast modulated patch or a patch of drifting grating elicited responses. A variety of patch sizes (0.5 to 1^{o}) were normally used for this test. They were presented in a randomized sequence over a set of spatial locations defined in rectangular coordinates. The location giving the largest response was used to define the center location, and the coordinates of the spatial locations adjusted to match. This involved several iterations with variations of patch size and stimulus coordinates to optimize both centering

and assessment of spatial extent. We then assessed area-summation using flashing spots, or patches of drifting grating, varying in diameter and presented in a randomized, interleaved manner. A typical example is shown in Fig. S1.

During the figure-ground task, the figure could appear in one of 4 equidistant positions away from the fixation spot; one of these positions was centered on the RF of the neuron(s) under study. Figure locations were varied in a randomized interleaved sequence. Apart from opposite direction of motion, the figure and ground random dot stimuli shared identical parameters: dot size subtended 0.1°, dot speed was 4°/s (dots moved 2.29 pixels/frame), dot density was a constant 25 dots/$^{\circ 2}$/s, dot coherence/correlation was 100% (50). All dots were spatially and positionally anti-aliased (see SI Experimental Procedures). Between every trial, individual dot position was fully randomized so no two trials exhibited the same spatial per-dot configuration. Each dot had a luminance chosen randomly on each trial from a uniform grayscale distribution between and inclusive of the darkest (0.02cd/m^{-2}) and brightest (65cd/m^{-2}) luminance values generated by the calibrated monitor. Overall mean background luminance was 32.4cd/m^{-2}. Dots were not limited lifetime (their kill rate was set to 0). Stimulus motion continued from motion onset until the monkey had successfully completed the task by making a saccade to and re-fixating at the figure center. To ensure we compared figure and ground conditions with identical stimulus parameters we collected data for both directions of motion of the figure and ground for each location (4 positions and 2 directions resulted in 8 trials per block). Animals normally performed 20 repeated blocks. The monkeys performed the task at approximately 80% accuracy overall, compared to a random response performance expectation of 25% (79.8 ± 1.25% SE, n = 91 and 83.4 ± 2.43% SE, n = 49, for each monkey respectively). Figure size was normally set

to 3 or 4° (in accordance with typical sizes used previously in V1 (38)) but was reduced in some cases to 2 or 2.5° to ensure the figure border was at least 1° away from the fixation point. This reduction in figure size did not impact on the results; there was no significant correlation between FGM magnitude and stimulus size (P = 0.430, R = -0.067, Spearman Rank R test).

Data analysis. Responses were only analyzed for correct trials. For each stimulus condition, responses were compiled into an average response histogram using a bin width of 10ms. We used the onset of motion to mark time-zero and computed background activity from a 200ms time epoch immediately prior to motion onset. For each cell, we computed the time to saccade initiation on a trial-by-trial basis, and restricted our analysis window across all trials to spikes that preceded the earliest saccade initiation time. We defined the average response for each stimulus type as the mean firing rate of the neuron for the period between response onset and this earliest saccade initiation time and calculated evoked responses by subtracting background activity. The response onset latency was defined as the first sampling window after motion onset where the firing rate exceeded background discharge rates by more than the 99% bootstrapped confidence interval (bias corrected and accelerated percentile method, BOOTCI, Matlab), provided it was followed immediately by at least two successive bins meeting this criterion. Cells were excluded from further analysis if neither the figure nor ground response as defined above exceeded the 99% bootstrapped confidence interval of the background activity level. Receptive fields were parafoveal and all located within 15° of the fovea, with >90% recorded within the central 10° (median eccentricity 7.0° ± 2.93 SD, n =140).

For each cell, we calculated a figure versus ground modulation index (FGM), calculated as: FGM = 100 * [($R_{figure} - R_{ground}$) / ($R_{figure} + R_{ground}$)] where R was the evoked response for the given condition. In accordance with previous work in V1 (3, 6, 38), we averaged the responses to both directions of motion, prior to computing the FGM index. Thus the figure and ground responses resulted from exposing the RF to the identical set of local features across trials (although 'ground' trials were three times more frequent) ensuring that our results were not influenced by any potential difference in the responses to the two directions of motion (due to the weak direction biases sometimes observed in macaque LGN cells (24)). We regarded cells that showed an FGM value greater than 20% as showing evidence of figure to ground response enhancement.

A potential concern was that a variation in the incidence of microsaccadic eye movements between figure and ground stimulation conditions could lead to a difference in neural responses. To detect microsaccades we used the velocity based algorithm code from Engbert and Mergenthaler, 2006 (51), see SI, Experimental Procedures. For each unit, we counted the number of microsaccades in the time epoch spanning 200ms prior to motion onset (our baseline time period) to the earliest saccade initiation time, for figure and ground stimulus conditions. We expressed the results as a ratio of the number of microsaccades per trial (in order to compensate for the difference in trial numbers for the two conditions). There was no significant difference (P = 0.145, Wilcoxon matched pairs test, n = 140) in the incidence of microsaccades between figure and ground stimulation conditions. There was also no significant correlation between FGM magnitude and microsaccade incidence (for either figure or ground stimuli) across our sample (P = 0.325, R = 0.085 and P = 0.677, R = 0.036 respectively for figure and ground conditions, Spearman Rank R test).

To construct average population histograms, we first normalized the smoothed (at 1.5 times the bin width) PSTH for individual neurons, after subtraction of background firing, to their maximum firing rate. Normalized responses of all neurons were then averaged. For individual data examples (eg Fig. 1) firing rate density functions were constructed by convolving the spike trains with a ±15ms Gaussian smoothing kernel, after exclusion of trials that included microsaccades occurring in the time epoch spanning from 200ms prior to figure onset to the end of the analysis time window. Unless otherwise indicated, for population statistics we used the median as a measure of central tendency and non-parametric two tailed tests for population data comparisons as the data were not normally distributed (Shapiro-Wilk normality test).

Acknowledgments

Supported by BBSRC grant G022305/1 & MRC grant G0701535. The research materials supporting this publication can be accessed from http://zenodo.org/record/11080 or by contacting either hjones@ioores.co.uk or a.sillito@ioores.co.uk.

References

1. Grossberg S, Mingolla E (1985) Neural dynamics of form perception: boundary completion, illusory figures, and neon color spreading. *Psychol Rev* 92:173-211.
2. Mumford D, Kosslyn SM, Hillger LA, Herrnstein RJ (1987) Discriminating figure from ground: the role of edge detection and region growing. *Proc Natl Acad Sci USA* 84:7354-7358.

3. Lamme VA, Supär H, Spekreijse H (1998) Feedforward, horizontal, and feedback processing in the visual cortex. *Curr Opin Neurobiol* 8:529-535.

4. Marcus DS, Van Essen DC (2002) Scene segmentation and attention in primate cortical areas V1 and V2. *J Neurophysiol* 88:2648-2658.

5. Pessoa L, De Weerd P eds (2003) *Filling in. From perceptual completion to cortical reorganization* (Oxford University Press, New York).

6. Poort J*, et al.* (2012) The role of attention in figure-ground segregation in areas V1 and V4 of the visual cortex. *Neuron* 75:143-156.

7. Sillito AM, Cudeiro J, Jones HE (2006) Always returning: feedback and sensory processing in visual cortex and thalamus. *Trends Neurosci* 29:307-316.

8. Gilbert CD, Sigman M (2007) Brain states: top-down influences in sensory processing. *Neuron* 54:677-696.

9. Briggs F, Usrey WM (2011) Corticogeniculate feedback and visual processing in the primate. *J Physiol (Lond)* 589:33-40.

10. Sillito AM, Jones HE, Gerstein GL, West DC (1994) Feature-linked synchronization of thalamic relay cell firing induced by feedback from the visual cortex. *Nature* 369:479-482.

11. Jones HE*, et al.* (2012) Differential feedback modulation of center and surround mechanisms in parvocellular cells in the visual thalamus. *J Neurosci* 32:15946-15951.

12. Gulyas B, Lagae L, Eysel U, Orban GA (1990) Corticofugal feedback influences the responses of geniculate neurons to moving stimuli. *Exp Brain Res* 79:441-446.

13. Briggs F, Usrey WM (2009) Parallel processing in the corticogeniculate pathway of the macaque monkey. *Neuron* 62:135-146.

14. Suga N, Xiao Z, Ma X, Ji W (2002) Plasticity and corticofugal modulation for hearing in adult animals. *Neuron* 36:9-18.

15. McCormick DA, Von Krosigk M (1992) Corticothalamic activation modulates thalamic firing through glutamate "metabotropic" receptors. *Proc Natl Acad Sci USA* 89:2774-2778.

16. Marrocco RT, McClurkin JW, Young RA (1982) Modulation of lateral geniculate nucleus cell responsiveness by visual activation of the corticogeniculate pathway. *J Neurosci* 2:256-263.

17. Raudies F, Neumann H (2010) A neural model of the temporal dynamics of figure-ground segregation in motion perception. *Neural Networks* 23:160-176.

18. Barnes T, Mingolla E (2013) A neural model of visual figure-ground segregation from kinetic occlusion. *Neural Networks* 37:141-164.

19. Hupe JM*, et al.* (2001) Feedback connections act on the early part of the responses in monkey visual cortex. *J Neurophysiol* 85:134-145.

20. Rossi AF, Desimone R, Ungerleider LG (2001) Contextual modulation in primary visual cortex of macaques. *J Neurosci* 21:1698-1709.

21. Self MW, van Kerkoerle T, Super H, Roelfsema PR (2013) Distinct roles of the cortical layers of area V1 in figure-ground segregation. *Curr Biol* 23:2121-2129.

22. Dow BM (1974) Functional classes of cells and their laminar distribution in monkey visual cortex. *J Neurophysiol* 37:927-946.

23. Blasdel GG, Fitzpatrick D (1984) Physiological organization of layer 4 in macaque striate cortex. *J Neurosci* 4:880-895.

24. Lee BB, Creutzfeldt OD, Elepfandt A (1979) The responses of magnocellular and parvocellular cells of the monkey's lateral geniculate body to moving stimuli. *Exp Brain Res* 35:547-557.

25. Carrasco M (2011) Visual attention: the past 25 years. *Vision Res* 51:1484-1525.

26. Wiesel TN, Hubel DH (1966) Spatial and chromatic interactions in the lateral geniculate body of the rhesus monkey. *J Neurophysiol* 29:1115-1156.

27. Jones HE, Sillito AM (1991) The length-response properties of cells in the feline dorsal lateral geniculate nucleus. *J Physiol (Lond)* 444:329-348.

28. Sceniak MP, Chatterjee S, Callaway EM (2006) Visual spatial summation in macaque geniculocortical afferents. *J Neurophysiol* 96:3474-3484.

29. Lamme VA (1995) The neurophysiology of figure-ground segregation in primary visual cortex. *J Neurosci* 15:1605-1615.

30. Jones HE*, et al.* (2013) Responses of primate LGN cells to moving stimuli involve a constant background modulation by feedback from area MT. *Neurosci* 246:254-264.

31. Allman JM, Miezin FM, McGuinness ER (1985) Stimulus specific responses from beyond the classical receptive field: Neurophyysiological mechanisms for local-global comparisons in visual neurons. *Annu Rev Neurosci* 8:407-430.

32. Webb BS*, et al.* (2002) Feedback from V1 and inhibition from beyond the classical receptive field modulates the responses of neurons in the primate lateral geniculate nucleus. *Visual Neurosci* 19:583-592.

33. Solomon SG, White AJR, Martin PR (2002) Extraclassical receptive field properties of parvocellular, magnocellular, and koniocellular cells in the primate lateral geniculate nucleus. *J Neurosci* 22:338-349.

34. Cudeiro J, Sillito AM (1996) Spatial frequency tuning of orientation-discontinuity-sensitive corticofugal feedback to the cat lateral geniculate nucleus. *J Physiol (Lond)* 490:481-492.

35. Allman J, Miezin F, McGuinness E (1985) Direction- and velocity-specific responses from beyond the classical receptive field in the middle temporal visual area (MT). *Perception* 14:105-126.

36. Knierim JJ, Van Essen DC (1992) Neuronal responses to static texture patterns in area V1 of the alert macaque monkey. *J Neurophysiol* 67:961-980.

37. Sillito AM, Grieve KL, Jones HE, Cudeiro J, Davis J (1995) Visual cortical mechanisms detecting focal orientation discontinuities. *Nature* 378:492-496.

38. Zipser K, Lamme VAF, Schiller PH (1996) Contextual modulation in primary visual cortex. *J Neurosci* 16:7376-7389.

39. Supèr H, Spekreijse H, Lamme VaF (2003) Figure–ground activity in primary visual cortex (V1) of the monkey matches the speed of behavioral response. *Neuroscience Letters* 344:75-78.

40. Reppas JB, Usrey WM, Reid RC (2002) Saccadic eye movements modulate visual responses in the lateral geniculate nucleus. *Neuron* 35:961-974.

41. Carrasco M, Evert DL, Chang I, Katz SM (1995) The eccentricity effect: target eccentricity affects performance on conjunction searches. *Percept Psychophys* 57:1241-1261.

42. McAlonan K, Cavanaugh J, Wurtz R (2008) Guarding the gateway to cortex with attention in visual thalamus. *Nature* 456:391-394.

43. Roelfsema PR, Tolboom M, Khayat PS (2007) Different processing phases for features, figures, and selective attention in the primary visual cortex. *Neuron* 56:785-792.

44. Regan D, Beverley KI (1984) Figure-ground segregation by motion contrast and by luminance contrast. *J Opt Soc Am A Opt Image Sci Vis* 1:433-442.

45. Lisberger SG, Movshon JA (1999) Visual motion analysis for pursuit eye movements in area MT of macaque monkeys. *J Neurosci* 19:2224-2246.

46. O'Connor DH, Fukui MM, Pinsk MA, Kastner S (2002) Attention modulates responses in the human lateral geniculate nucleus. *Nature Neurosci* 5:1203-1209.

47. Anderson EJ, Dakin SC, Rees G (2009) Monocular signals in human lateral geniculate nucleus reflect the Craik-Cornsweet-O'Brien effect. *J Vis* 9:14 11-18.

48. Malpeli JG, Baker FH (1974) The representation of the visual field in the lateral geniculate nucleus of macaca mulatta. *J Comp Neurol* 161:569-594.

49. Bender DB (1981) Retinotopic organization of macaque pulvinar. *J Neurophysiol* 46:672-693.

50. Britten KH, Shadlen MN, Newsome WT, Movshon JA (1992) The analysis of visual motion: A comparison of neuronal and psychophysical performance. *J Neurosci* 12:4745-4765.

51. Engbert R, Mergenthaler K (2006) Microsaccades are triggered by low retinal image slip. *Proc Natl Acad Sci U S A* 103:7192-7197.

Figure Legends

Fig. 1. Enhancement of neuronal firing when the figure, as opposed to the ground component of the stimulus, was located over the RF. (A-B) Schematic depiction (not to scale) of the stimulus and behavioral paradigm. The full screen random dot display was initially static, with a central, yellow fixation spot (A). After a minimum fixation period of 400 ms, motion initiated. A single square figure, delineated solely by its opposite direction of dot motion, was visible at one of four possible locations (indicated here by green/blue squares) either centered over the RF (depicted by the red circle) as shown in the upper panel or at an alternative location as shown in the lower panel (B). Monkeys were rewarded for making a saccade (within 500ms of motion onset) to the center of the figure target. (C-F) Responses of 4 example LGN neurons. Spike density functions (SDF) to ground (black) and figure (red) stimulus conditions (±1SE). Inset schematics show the size of the RF relative to the figure size. Time epoch commences 50ms prior to stimulus motion onset and ends prior to saccade initiation. See also Fig. S1.

Fig. 2. Population summary data. (A) Averaged population responses to figure (red) and ground (black) stimulus conditions overlying the RF. Shading represents ± 1 SE. Motion onset occurred at time 0ms. Horizontal dotted line denotes background plus 99% confidence limit. See Materials and Methods, (last paragraph) for full details of the normalization procedure. (B) Bar group-histogram plots the distribution of FGM (in %) across our sample for multi-units (Mu, black), Parvocellular (P, red), Magnocellular (M, green), and Koniocellular (K, blue) cells. The median FGM was 56% ± 6.07 SE, n = 140. The FGM values for each monkey were 60% (± 5.69 SE, n = 91) and 45% (± 12.84 SE, n =

49) respectively. There was no significant difference between the FGM values observed for the two monkeys for either the single unit data, multi unit data or combined single and multi unit data sets ($P > 0.05$ for each comparison, Wilcoxon matched pairs test). Our single unit population sample was largely comprised of parvocellular (P) cells (n = 60) although we also obtained some recordings from both koniocellular (K, n = 8) and magnocellular (M, n = 9) cells. Across our single unit data, there was no significant difference in either the magnitude of the FGM index ($P = 0.7172$, Kruskal-Wallis ANOVA) or proportion of cells exhibiting the effect ($P = 0.118$, Freeman Halton extension of Fisher Exact Probability test) across the three cell groups. (C) Box-notch plots of figure (left) and ground (right) responses (in s/s after subtraction of background activity). The horizontal line in the middle of the box shows the median response and the notch limits signify the 95% confidence interval around the median; box limits signify 25th and 75th percentiles of the data, and the extended whiskers show 1.5 times the interquartile range. Responses outside a range 1.5 times the width of the inter-quartile range from the median are shown as separate points (red crosses). The two notches do not overlap vertically, thus the corresponding medians are different at the 5% level. (D) Distribution of ground responses versus figure responses (in s/s after subtraction of background activity) across the cell sample. Dashed line denotes the diagonal representing equal responses to both stimuli. Negative values represent cases where responses to ground stimulation were reduced below the background firing rate (27). Color conventions as in Fig. 2B.

Fig. 3. Comparison of responses to figure and border stimuli located over the RF. (A-B) SDFs for two example LGN cells to conditions where the border (blue) or figure (red) was

present over the RF. Conventions as in Fig. 1C-F. (C) Population summary data plotting the averaged population responses to figure (red) and border (blue) stimulus conditions overlying the RF (n = 37). Horizontal dotted line denotes background plus 99% confidence limit. Conventions as in Fig. 2A.

Fig. 4. Enhancement of neuronal firing to a figure located over the RF in the absence of saccades. (A-B) SDFs for two example LGN cells to ground (black) and figure (red) stimulus conditions overlying the RF. Diagrammatic conventions as in Fig. 1C-F. As for our standard stimulus paradigm, the full screen random dot display was initially static, with a central, yellow fixation spot. After a minimum fixation period of 400 ms, motion initiated and a single square figure, delineated solely by its opposite direction of dot motion, was visible at one of four possible locations. As the RFs of these cells were located very near the fovea, when the figure was centered over the RF, it encompassed the fixation window and the monkey was rewarded for maintaining fixation. When the stimulus was located at one of the three alternative locations displaced from the RF (and arranged in similar locations to those normally occupied by the non-receptive field figure locations in our standard paradigm) monkeys were rewarded for making a saccade (within 500ms of motion onset) to the center of the figure target as normal. (C) Population summary data plotting the averaged population responses to figure (red) and ground (black) stimulus conditions overlying the RF (n = 20). Horizontal dotted line denotes background plus 99% confidence limit. Conventions as in Fig. 2A. (D) Box-notch plots of figure (left) and ground (right) responses (in s/s after subtraction of background activity). The horizontal line in the middle of the box shows the median response and the notch limits signify the

95% confidence interval around the median; box limits signify 25th and 75th percentiles of the data, and the extended whiskers show 1.5 times the interquartile range. Responses outside a range 1.5 times the width of the inter-quartile range from the median are shown as separate points (red crosses). The two notches do not overlap vertically, thus the corresponding medians are different at the 5% level.

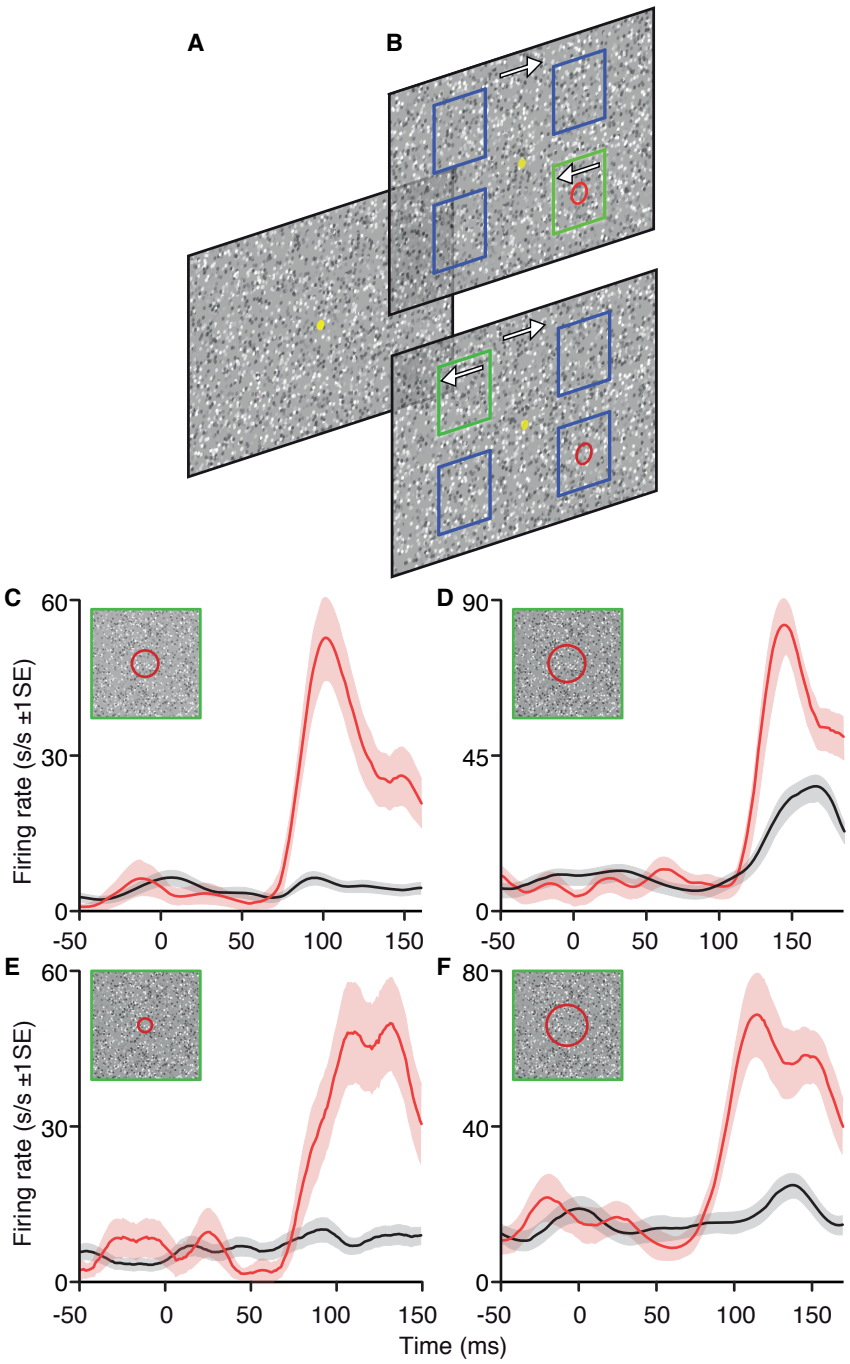
A
B
C
D
E
F
Firing rate (s/s ±1SE)
Time (ms)
60
30
0
90
45
80
40
-50
0
50
100
150

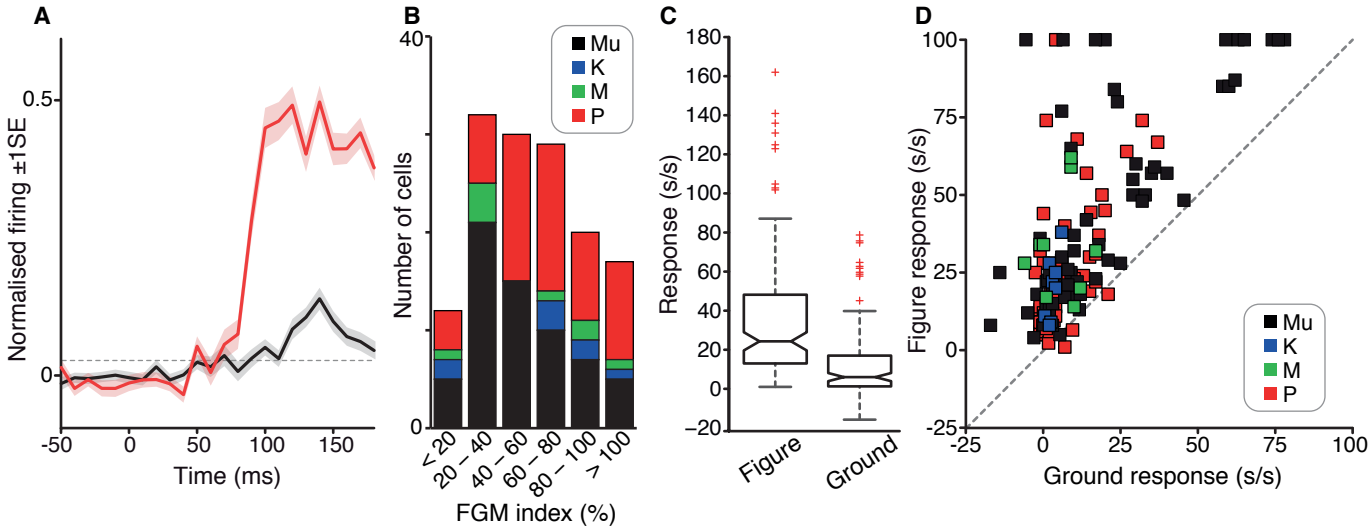
A
Normalised firing ±1SE
0.5
0
-50
0
50
100
150
Time (ms)
B
Number of cells
40
0
Mu
K
M
P
< 20
20 – 40
40 – 60
60 – 80
80 – 100
> 100
FGM index (%)
C
Response (s/s)
180
160
140
120
100
80
60
40
20
0
–20
Figure
Ground
D
Figure response (s/s)
100
75
50
25
0
-25
-25
0
25
50
75
100
Ground response (s/s)
Mu
K
M
P

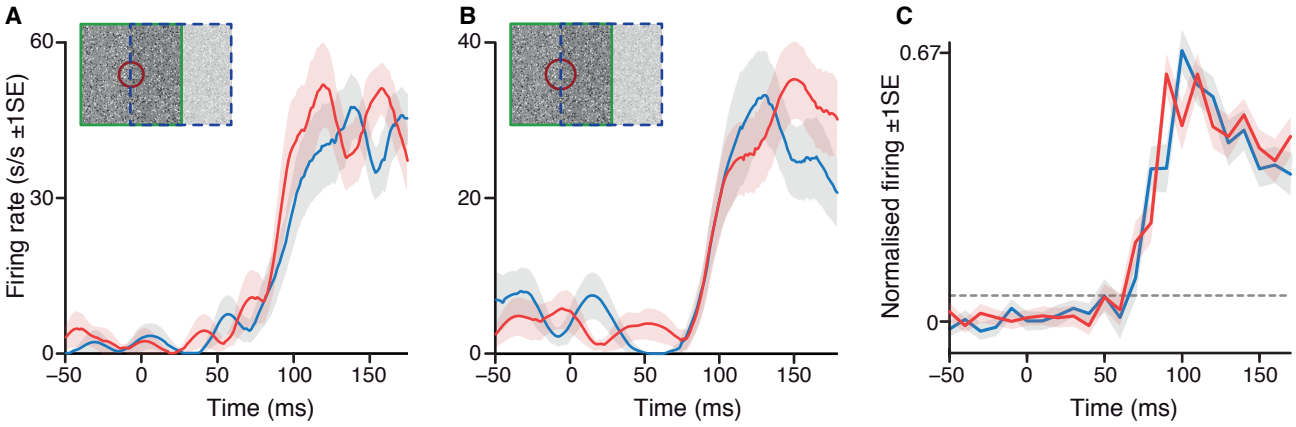
A
60
30
0
Firing rate (s/s ±1SE)
–50
0
50
100
150
Time (ms)
B
40
20
0
–50
0
50
100
150
Time (ms)
C
0.67
0
Normalised firing ±1SE
–50
0
50
100
150
Time (ms)

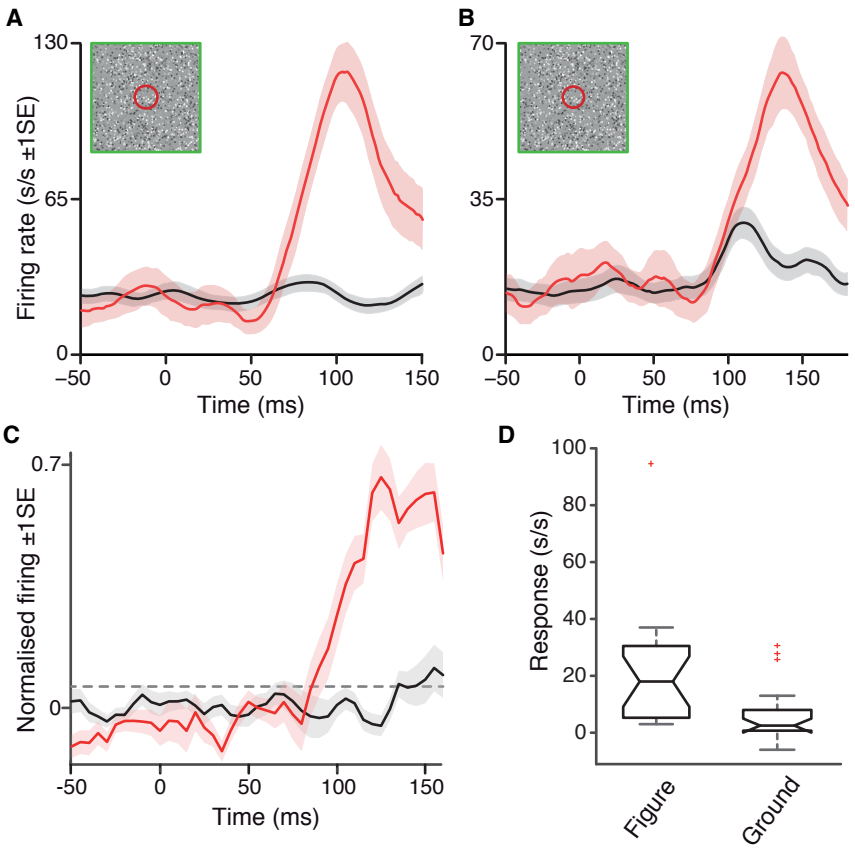
A
130
65
0
Firing rate (s/s ±1SE)
–50
0
50
100
150
Time (ms)
B
70
35
0
–50
0
50
100
150
Time (ms)
C
0.7
0
Normalised firing ±1SE
-50
0
50
100
150
Time (ms)
D
100
80
60
40
20
0
Response (s/s)
Figure
Ground